P H Y S I C A L   R E V I E W   L E T T E R S

A Universal Criterion for Plastic Yielding of Metallic Glasses with a $(T/T_g)^{2/3}$ Temperature Dependence

W. L. Johnson[*] and K. Samwer[†]

138-78 Keck Laboratory of Engineering, California Institute of Technology, Pasadena, California 91125, USA
(Received 25 January 2005; published 3 November 2005)

Room temperature (T_R) elastic constants and compressive yield strengths of ~ 30 metallic glasses reveal an average shear limit $\gamma_C = 0.0267 \pm 0.0020$, where $\tau_Y = \gamma_C G$ is the maximum resolved shear stress at yielding, and G the shear modulus. The γ_C values for individual glasses are correlated with $t = T_R/T_g$, and γ_C for a single glass follows the same correlation (vs $t = T/T_g$). A cooperative shear model, inspired by Frenkel's analysis of the shear strength of solids, is proposed. Using a scaling analysis leads to a universal law $\tau_{CT}/G = \gamma_{C0} - \gamma_{C1}(t)^{2/3}$ for the flow stress at finite T where $\gamma_{C0} = (0.036 \pm 0.002)$ and $\gamma_{C1} = (0.016 \pm 0.002)$.

For a dislocation free crystal, Frenkel [1] calculated the theoretical shear strength by assuming cooperative shearing obtaining $\tau_Y \cong G/5$. The yield strength of metallic glasses is thought to be determined by the cooperative shear motion of atomic clusters termed shear transformation zones (STZ's) [2–5]. Compressive strengths of $\sigma_Y \sim 0.02Y$ are observed with a weak dependence on normal stress or pressure [6,7]. Here, we report elastic constants and compressive yield stresses for ~ 30 metallic glasses. Yielding at T_R can be described by a critical shear strain $\gamma_C = 0.0267 \pm 0.0020$; a better description of γ_C includes a dependence on the dimensionless temperature $t = T/T_g$. A cooperative shear model (CSM) is introduced that predicts a temperature dependent τ_C (or γ_C) having a "$T^{2/3}$" form. The CSM is based on the concept of inherent states (IS) and potential energy landscapes (PEL) developed by Stillinger *et al.* [8,9], Wales *et al.* [10,11], and Milandro and Lacks [12].

Table I shows measured density, ambient T elastic constants Y, G, B, ν (Poisson's ratio), yield strength in compression, σ_y, elastic strain limit (σ_Y/Y), and glass transition temperature, T_g, for ~ 30 metallic glasses [13–29]. Note that σ_Y/Y varies over the range $0.014 < \varepsilon_Y < 0.022$. Ignoring the small normal stress dependence of the shear yield strength [6,7,13,14], one can plot τ_Y vs G $(\tau_Y = \sigma_Y/2)$ to find the corresponding elastic shear strain limit as shown in Fig. 1. We obtain linear correlation with a best fit of $\gamma_C = \tau_Y/G = 0.0267 \pm 0.0020$, but there remains significant scatter in γ_C. Examination shows that glasses with low T_g tend to exhibit smaller γ_C than those with high T_g. Consider the reduced temperature, $t = T_R/T_g$. We plot γ_C for each individual alloy vs t (open circles) in Fig. 2. The plot includes data (filled circles) for the temperature dependent τ_Y of Vitreloy 1 (fixed T_g and varying T) by Lu *et al.* [13], low temperature data for bulk La$_{55}$Al$_{25}$Cu$_{20}$ [30] (squares), melt spun ribbons of Pd$_{85.5}$Si$_{14.5}$ [31] (stars), and Fe$_{40}$Ni$_{40}$P$_{14}$B$_6$ [31] (horizontal triangles), and bulk Pd$_{77.5}$Cu$_6$Si$_{16.5}$ [2(b),24] (vertical triangles). The data for ribbons were "normalized" to obtain

agreement with other data at $T = 0$ K (G was not known for the ribbons). The "peak flow stress" of Vitreloy 1 vs T (from T_R to above T_g) was taken as τ_Y. Figure 2 shows that γ_C is a systematic function of t.

Following Frenkel, the elastic energy of an STZ is here described by a periodic elastic energy density vs strain:

$$\phi(\gamma) = \phi_0/2[1 - \cos(\pi\gamma/2\gamma_C)] = \phi_0 \sin^2(\pi\gamma/4\gamma_C) \quad (1)$$

with a minima at $\gamma = 0$, a barrier at $2\gamma_C$ (γ_C is the yield strain), and a total barrier energy density ϕ_0. The critical yield stress is $\phi'|_{\max} = \tau_c = \pi\phi_0/4\gamma_C$. For the unstressed solid, $G = \phi''|_{\gamma=0}$ giving $\phi_0 = (8/\pi^2)G\gamma_C^2$. The "free enthalpy" density of the stressed STZ is $h(\gamma) = \phi(\gamma) - \tau\gamma$. In an unstressed solid, the total potential energy barrier for an STZ is $W = \phi_0\zeta\Omega = (8/\pi^2)G\gamma_C^2\zeta\Omega$, where Ω is the actual volume of the STZ defined by the plastic "core," and ζ is a correction factor arising from matrix confinement of a "dressed" STZ [2,32]. For a Gaussian shaped strain fluctuation with core diameter σ, one can estimate $\zeta \sim 2$–4 and $W \sim 3\Omega\phi_0$. The details of ζ depend on the shape and size of the fluctuation and the elastic constants G and ν for the material.

For an infinite crystal of indistinguishable atoms, the periodic minima of $\phi(\gamma)$ are equivalent; i.e., there is no configurational entropy. For a glass, there are Γ stable atomic configurations or inherent states (IS's) [8,9,33] with $\Gamma = \exp(N\Delta s_C)$, where N is the number of atoms in the STZ, and Δs_C the configurational entropy per atom of the IS's or "basin denumeration function" [9,33]. While Δs_C is well defined in the thermodynamic limit $N \to \infty$, it decreases [9,10,33] for small N. The characteristic strain (γ_C) or "configurational displacement" separating neighboring configurations will increase for $N \sim 100$ or less. On the other hand, the total barrier W also scales with STZ volume Ω (or N). Therefore $W \sim \gamma_C^2\Omega$ is expected have a minimum for some intermediate N^*. We estimate that N^* is likely of order ~ 100 atoms. Yielding occurs when the applied stress causes a critical density of "minimum" barrier STZ's to become unstable.

195501-1

TABLE I. Summary of data on alloy compositions and properties used in this Letter.

Alloy	ρ (g/cc)	Y) (GPa)	G (GPa)	B (GPa)	ν	σ_y (GPa)	T_g (K)	σ_y/Y	Ref.
1. $Zr_{41.2}Ti_{13.8}Ni_{10}Cu_{12.5}Be_{22.5}$	5.9	95	34.1	114.1	0.352	1.86	618	0.0196	[13–15]
		97.2	35.9	111.2	0.354	1.85	613	0.0190	
2. $Zr_{48}Nb_8Ni_{12}Cu_{14}Be_{18}$	6.7	93.9	34.3	118	0.367	1.95	620	0.0208	[15]
3. $Zr_{55}Ti_5Cu_{20}Ni_{10}Al_{10}$	6.62	85	31	118	0.375	1.63	625	0.0192	[15]
4. $Zr_{57.5}Nb_5Cu_{15.4}Ni_{12}Al_{10}$	6.5	84.7	30.8	117.6	0.379	1.58	663	0.0187	[15]
5. $Zr_{55}Al_{19}Co_{19}Cu_7$	6.2	101.7	37.6	114.9	0.352	2.2	733	0.0216	[16]
6. $Pd_{40}Cu_{30}Ni_{10}P_{20}$	9.28	92	34.5	151.8	0.399	1.72	593	0.0187	[17]
7. $Pd_{40}Cu_{30}Ni_{10}P_{20}$	9.28	92	33	146	0.394	1.72	593	0.0187	[18]
8. $Pd_{40}Cu_{30}Ni_{10}P_{20}$	9.30	92	35.8	144.7	0.394	1.75	595	0.0190	[17]
9. $Pd_{60}Cu_{20}P_{20}$	9.78	91	32.3	167	0.409	1.70	604	0.0187	[15]
10. $Pd_{40}Cu_{40}P_{20}$	9.30	93	33.2	158	0.402	1.75	548	0.0188	[15]
11. $Ni_{45}Ti_{20}Zr_{25}Al_{10}$	6.4	109.3	40.2	129.6	0.359	2.37	791	0.0217	[19]
12. $Ni_{40}Ti_{17}Zr_{28}Al_{10}Cu_5$	6.48	127.6	47.3	140.7	0.349	2.59	862	0.0203	[19]
13. $Ni_{60}Nb_{35}Sn_5$	8.64	183.7	66.32	267	0.385	3.85	885	0.0210	[20]
14. $Ni_{60}Sn_6(Nb_{0.8}Ta_{0.2})_{34}$	9.24	161.3	59.41	189	0.357	3.50	875	0.0217	[16]
15. $Ni_{60}Sn_6(Nb_{0.6}Ta_{0.4})_{34}$	9.80	163.7	60.1	197.6	0.361	3.58	882	0.0219	[16]
16. $Cu_{64}Zr_{36}$	8.07	92	34	104.3	0.352	2.0	787	0.0217	[21]
17. $Cu_{46}Zr_{54}$	7.62	83.5	30.0	128.5	0.391	1.40	696	0.0168	[22]
18. $Cu_{46}Zr_{42}Al_7Y_5$	7.23	84.6	31	104.1	0.364	1.60	713	0.0189	[23]
19. $Pd_{77.5}Cu_6Si_{16.5}$	10.4	89.7	31.8	166	0.409	1.5	550	0.0167	[24]
20. $Pt_{60}Ni_{15}P_{25}$	15.7	96.1	33.8	202	0.420	1.4	488	0.0146	[25]
21. $Pt_{57.5}Cu_{14.7}Ni_5P_{22.8}$	15.2	95.7	33.4	243.2	0.434	1.45	490	0.0151	[26]
22. $Pd_{64}Ni_{16}P_{20}$	10.1	91.9	32.7	166	0.405	1.55	452	0.0169	[24]
23. $MgGd_{10}Cu_{25}$	4.04	49.1	18.6	46.3	0.32	0.98	428	0.020	[16]
24. $La_{55}Al_{25}Cu_{10}Ni_5Co_5$	6.0	41.9	15.6	44.2	0.342	0.85	430	0.0203	[15]
25. $Ce_{70}Al_{10}Ni_{10}Cu_{10}$	6.67	30.3	11.5	27	0.313	0.65	359	0.0215	[27]
26. $Cu_{50}Hf_{43}Al_7$	11.0	113	42	132.8	0.358	2.2	774	0.0195	[16]
27. $Cu_{57.5}Hf_{27.5}Ti_{15}$	9.91	103	37.3	117.5	0.356	1.94	729	0.0188	[16]
28. $Fe_{61}Mn_{10}Cr_4Mo_6Er_1C_{15}B_6$	6.89	193	75	146	0.280	4.16	870	0.0216	[28]
29. $Fe_{53}Cr_{15}Mo_{14}Er_1C_{15}B_6$	6.92	195	75	180	0.32	4.2	860	0.0215	[28]
30. $Au_{49.5}Ag_{5.5}Pd_{2.3}Cu_{26.9}Si_{16.3}$	11.6	74.4	26.5	132.3	0.406	1.20	405	0.0141	[29]
31. $Au_{55}Cu_{25}Si_{20}$	12.2	69.8	24.6	139.8	0.417	1.00	348	0.0143	[29]

The barrier at finite τ, W_τ, approaches zero as $\tau \to \tau_C$. It is easily shown that $\phi_{0\tau}$ (barrier energy density at finite $\tau \to \tau_C$) decreases as $\phi_{0\tau} \sim (\tau_C - \tau)^{3/2}$ while the shear modulus (at finite τ) $G_\tau \sim (\tau_C - \tau)^{1/2}$. The strain difference between the energy minimum and barrier configuration (saddle point) scales as $\delta\gamma_\tau \sim (\tau_C - \tau)^{1/2}$ as $\tau \to \tau_C$. Mechanical instability of the STZ at τ_C takes the form of a "fold catastrophe" [11,34]. For $\tau \to \tau_C$, the parameters $W_\tau = \phi_{0\tau}\zeta\Omega$, $\delta\gamma_\tau$, and G_τ, are related by the scaling law

$$\phi_{0\tau}/(G_\tau(\delta\gamma_\tau)^2) = R = 1/4,$$
$$\text{so that } W_\tau = G_\tau\gamma_{C\tau}^2\zeta\Omega, \quad (2)$$

where R is the "fold ratio." Wales *et al.* [11,34] have shown that, for binary Lennard Jones (LJ) glasses (256 atoms) and liquid salt clusters (71 atoms), this scaling relation holds *on average,* even far from τ_C. For the Frenkel landscape of Eq. (1), R actually varies from 1/4

to $\pi^2/32$ as τ varies from τ_C down to 0. Analysis of simulation results [12] for shear induced destabilization of individual IS's of a 500 atom LJ glass shows that Eq. (2) is obeyed (within 10%) over $0 < \tau < \tau_C$. Assuming scaling holds on average:

$$W_\tau = W_0(T)[(\tau_C - \tau)/\tau_C]^{3/2} = \phi_0[(\tau_C - \tau)/\tau_C]^{3/2}\zeta\Omega$$
$$= 4RG_{0T}\gamma_C^2[(\tau_C - \tau)/\tau_C]^{3/2}\zeta\Omega, \quad (3)$$

where G_{0T} is the shear modulus of the *unstressed glass* which includes a *weak* dependence on T (Debye-Grüneisen thermal expansion) for a fixed glass configuration. The scaling law holds for any function $\phi(\gamma)$ for which $d^2\phi(\gamma)/d\gamma^2$ is analytic around the inflection point. At finite T and applied τ, thermal strain fluctuations will carry the system over the barrier W_τ. For plastic flow to occur on a given time scale (or strain rate $\dot\gamma$), the rate of barrier crossing must reach a critical value comparable to $\dot\gamma$. Using

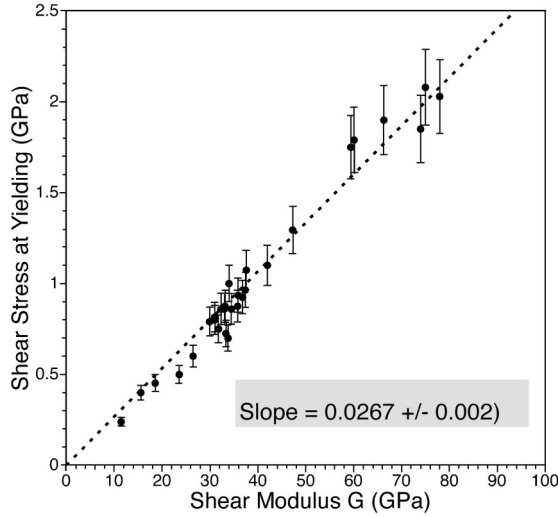FIG. 1. Experimental shear stress at yielding, $\tau_Y = \sigma_Y/2$ vs shear modulus G at room temperature for 30 bulk metallic glasses.
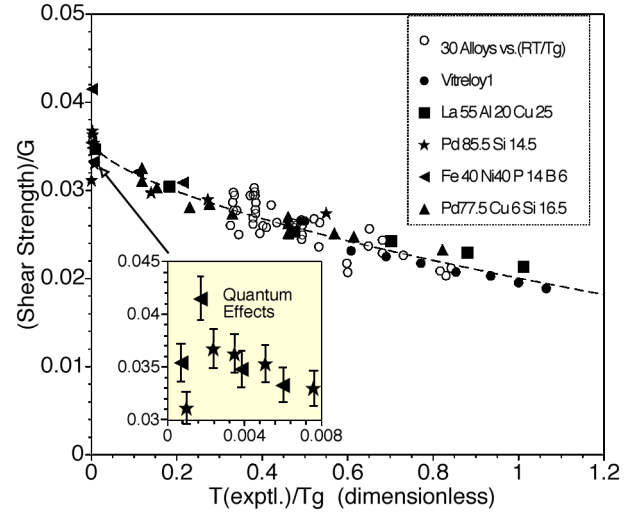

FIG. 2 (color online). Experimental shear strain at yielding (τ_Y/G) vs $t = T/T_g$. Small open circles show results at room temperature on 30 alloys of varying T_g. Solid symbols show the t dependence of τ_Y/G for various individual alloys as indicated. The reader is referred to the text for references and details.

an attempt frequency ω_0 requires

$$\text{yielding rate} = \omega_0 \exp(-W_\tau/kT) = C\dot{\gamma}, \qquad (4)$$

with C a dimensionless constant of order unity, and thus

$$W_\tau/kT = -\ln(C\dot{\gamma}/\omega_0)$$
$$= \{4RG_{0T}\gamma_C^2[(\tau_{C0} - \tau_{CT})/\tau_C]^{3/2}\zeta\Omega\}/kT. \quad (5)$$

Here, τ_{C0} is the yield stress at $T = 0$, while τ_{CT} is at finite T. One obtains

$$\tau_{CT} = \tau_{C0} - \tau_{C0}[kT\ln(\omega_0/C\dot{\gamma})/(4RG_{0T}\gamma_C^2\zeta\Omega)]^{2/3}. \quad (6)$$

At $T = T_g$ and $\tau = 0$, the barrier is $W_0(T_g) = 4RG_{0Tg}\gamma_C^2\zeta\Omega$. If T_g itself is defined by a critical barrier crossing rate due to fluctuations, one obtains $W_0(T_g) = \beta T_g$, with β constant. This yields

$$W_{\tau,Tg} = \beta T_g[(\tau_C - \tau)/\tau_C]^{3/2}. \qquad (7)$$

Equation (6) for the yield stress becomes

$$\tau_{CT} = \tau_{C0} - \tau_{C0}[(k/\beta)\ln(\omega_0/C\dot{\gamma})(G_{0T}/G_{0Tg})]^{2/3}t^{2/3}, \quad (8)$$

where $t = T/T_g$. The factor (G_{0T}/G_{0Tg}) incorporates the weak dependence of G on the thermal expansion of a fixed glass configuration. G_{0T} has been experimentally determined [15,18] to be a linear function of T. For Vitreloy 1 [15], one finds $dG_{0T}/dT \sim 4 \times 10^{-3}$ (GPa/K) with $G_0 \sim 37$ GPa at 0 K. Since the thermal expansion coefficient will drop at very low T, one obtains an upper bound for the fractional change in (G_{0T}/G_{0Tg}) from 0 K to T_g as $\Delta_{\max} = (T_g/G_0)(dG_{0T}/dT) \sim 0.07$. Similarly, we estimate $\Delta_{\max} \sim 0.11$ for $Pd_{40}Ni_{40}P_{20}$ [18]. The t dependence of (G_{0T}/G_{0Tg}) gives a maximum correction to the second term in Eq. (8)

at $t \sim 1$ (near T_g) of order 5%–7%. The logarithmic term in Eq. (8) involves ω_0 and is estimated to be the frequency of shear phonon of nm wavelength ($\sim 10^{13}$ Hz). With typical strain rates (in yielding experiments) of 10^{-2}–10^{-4} s^{-1}, we have $\ln(\omega_0/C\dot{\gamma}) \sim 30$. An order of magnitude change in either ω_0 or $\dot{\gamma}$ changes the logarithmic term by $\sim 5\%$. The dependence of τ_{CT} on T is thus dominated by the $t^{2/3}$ term.

The dotted curve in Fig. 2 was obtained using Eq. (8) (square bracket taken as a constant) to "fit" the dependence of τ_{CT} at T_R (fixed T) and varying T_g for the 30 metallic glasses (open circles) and the t dependence of individual alloys (filled symbols). This fit gives $\tau_Y/G = \gamma_{C0} + \gamma_{C1}t^m$ where $\gamma_{C0} = 0.036 \pm 0.002$, $\gamma_{C1} = 0.016 \pm 0.002$, and $m = 0.62 \pm 0.2$. Equation (8) explains both the T dependence of τ_Y for all individual amorphous alloys and the "T_g dependence" for 30 glasses at fixed T_R with an exponent "m" consistent (within error) with the predicted value "2/3." The coefficients γ_{C0} and γ_{C1} are approximately universal constants. The present classical model is expected to break down at very low T. Low T data shown in the inset of Fig. 2 suggest "quantum effects" on yielding when shear phonon modes "freeze out" at very low T.

For the CSM, the elastic response of an STZ is nonlinear as τ increases from 0 to τ_C. The actual critical strain at τ_C is not τ_{CT}/G (as in experiments), but rather $\pi\tau_{CT}/2G$ with the factor $\pi/2$ arising from nonlinear elasticity. The role of nonlinear elasticity and nonaffine atomic displacements in the shear response of an STZ has been recently discussed [35,36]. In both the Frenkel model and simulations [35], the compliance at finite stress, G_τ^{-1}, diverges at τ_C. Experimentally, one measures yield stress, not strain,

so the experimental γ_C at yield underestimates the actual strain of the STZ. Further, the macroscopic material comprises a statistical distribution of STZ's with distributed values of G and τ_C varying with location and orientation. Yielding is expected when a critical fraction of unstable STZ's results in global instability.

In conclusion, plastic yielding of metallic glasses at T_R is roughly described by an average elastic shear limit criterion, $\tau_Y = \gamma_C G$, where G is the shear modulus of the unstressed glass, and $\gamma_C = 0.0267 \pm 0.0020$. Closer analysis reveals that γ_C depends on $t = T/T_g$. A CSM inspired by Frenkel's work and recent molecular dynamics simulations is developed to explain these empirical findings. Yielding is treated as a fold catastrophe obeying a scaling law $W(\tau)/[G_\tau(\delta\gamma)^2] = R$. Applied on average, this scaling law leads to a "$t^{2/3}$ law," $\tau_{CT}/G = \gamma_{C0} - \gamma_{C1}(t)^{2/3}$, for flow stress of metallic glasses where γ_{C0} and γ_{C1} are weakly material dependent. A fit to all experimental data yields $\gamma_{C0} = (0.036 \pm 0.002)$, $\gamma_{C1} = (0.016 \pm 0.002)$, and an exponent $m = 0.62 \pm 0.2$. A similar derivation of the "$T^{2/3}$" law has appeared in the literature on yielding in crystals [37]. Gaunt also derived a similar law for thermally activated domain wall motion in disordered magnets [38]. To the extent that plastic yielding in nonmetallic glasses (oxides, molecular glasses, etc.) is a fold catastrophe, one might expect Eq. (8) to be valid more generally although γ_{C0} may vary. The present CSM model may establish a basis for a broader understanding of glass physics.

---

*Electronic address: wlj@caltech.edu
†Permanent address: I. Physik Institute, University of Goettingen, Goettingen, Germany.

[1] J. Frenkel, Z. Phys. **37**, 572 (1926); see also A. Kelly, *Strong Solids* (Clarendon Press, Oxford, 1973), 2nd ed.
[2] (a) A. S. Argon, Acta Metall. **27**, 47 (1979); (b) A. Argon and L. T. Shi, Acta Metall. **31**, 499 (1983).
[3] F. Spaepen, Acta Metall. **25**, 407 (1977); see also P. S. Steif, F. Spaepen, and J. W. Hutchinson, Acta Metall. **30**, 447 (1982).
[4] M. L. Falk and J. S. Langer, Phys. Rev. E **57**, 7192 (1998).
[5] J. S. Langer, Phys. Rev. E **70**, 041502 (2004).
[6] See P. E. Donovan, Acta Metall. **37**, 445 (1989); J. J. Lewandowski and P. Lowhaphandu, Philos. Mag. A **82**, 3427 (2002).
[7] J. Lu and G. Ravichandran, J. Mater. Res. **18**, 2039 (2003).
[8] F. H. Stillinger and T. A. Weber, J. Chem. Phys. **88**, 7818 (1988); Science **267**, 1935 (1995).
[9] P. G. Debenedetti and F. H. Stillinger, Nature (London) **410**, 259 (2001).
[10] J. P. K. Doye and D. J. Wales, J. Chem. Phys. **116**, 3777 (2002).
[11] D. J. Wales, Science **293**, 2067 (2001).
[12] D. L. Malandro and D. J. Lacks, J. Chem. Phys. **110**, 4593 (1999); also **107**, 5804 (1997).
[13] J. Lu, G. Ravichandran, and W. L. Johnson, Acta Mater. **51**, 3429 (2003).
[14] H. Bruck, T. Christman, A. J. Rosakis, and W. L. Johnson, Scr. Metall. Mater. **30**, 429 (1994); also F. Szuecs, C. P. Kim, and W. L. Johnson, Acta Mater. **49**, 1507 (2001).
[15] Y. Zhang, D. Q. Zhao, R. J. Wang, and W. H. Wang, Acta Mater. **51**, 1971 (2003); also W. H. Wang, C. Dong, and C. H. Shek, Mater. Sci. Eng., R **44**, 45 (2004).
[16] J. Kang, M. L. Lind, H. C. Yim, and W. L. Johnson (unpublished).
[17] U. Harms, O. Jin, and R. B. Schwarz, J. Non-Cryst. Solids **317**, 200 (2003).
[18] N. Nishiyama, A. Inoue, and J. Z. Jiang, Appl. Phys. Lett. **78**, 1985 (2001).
[19] D. H. Xu, G. Duan, and W. L. Johnson, Acta Mater. **52**, 3493 (2004).
[20] H. Choi-Yim, D. H. Xu, and W. L. Johnson, Appl. Phys. Lett. **82**, 1030 (2003).
[21] D. H. Xu, B. Lohwongwatana, G. Duan, and W. L. Johnson, Acta Mater. **52**, 2621 (2004).
[22] G. Duan, D. H. Xu, and W. L. Johnson, Phys. Rev. B **71**, 224208 (2005).
[23] D. H. Xu, G. Duan, and W. L. Johnson, Phys. Rev. Lett. **92**, 245504 (2004).
[24] B. Golding, B. G. Bagley, and F. S. L. Hsu, Phys. Rev. Lett. **29**, 68 (1972).
[25] H. S. Chen, J. T. Krause, and E. Coleman, J. Non-Cryst. Solids **18**, 157 (1975).
[26] J. Schroers and W. L. Johnson, Appl. Phys. Lett. **84**, 3666 (2004); also Phys. Rev. Lett. **93**, 255506 (2004).
[27] B. Zhang, M. X. Pan, Q. Zhao, and W. H. Wang, Appl. Phys. Lett. **85**, 61 (2004).
[28] V. Ponnambalam, S. J. Poon, and G. J. Shiflet, J. Mater. Res. **19**, 3046 (2004); **19**, 1320 (2004); (private communication).
[29] J. Schroers, B. Lohwongwatana, A. Peker, and W. L. Johnson, Appl. Phys. Lett. **87**, 061912 (2005).
[30] S. Takeuchi, T. Kakegawa, T. Hashimoto, A.-P. Tsai, and A. Inoue, Mater. Trans., JIM **41**, 1443 (2000).
[31] V. Z. Bengus, E. D. Tabachnikova, P. Duhaj, and V. Ocelik, Mater. Sci. Eng. A **226–228**, 823 (1997).
[32] J. D. Eshelby, Proc. R. Soc. A **241**, 376 (1961).
[33] M. S. Shell, P. G. Debenedetti, W. LaNave, and F. Sciortino, J. Chem. Phys. **118**, 8821 (2003).
[34] T. V. Bogdan and D. J. Wales, J. Chem. Phys. **120**, 11 090 (2004).
[35] C. Maloney and A. Lemaitre, Phys. Rev. Lett. **93**, 195501 (2004).
[36] A. Tanguy, J. P. Wittmer, F. Leonforte, and J. L. Barrat, Phys. Rev. B **66**, 174205 (2002).
[37] U. F. Kocks, A. S. Argon, and M. F. Ashby, Prog. Mater. Sci. **19**, 1 (1975).
[38] P. Gaunt, Philos. Mag. B **48**, 261 (1983); Philos. Mag. **34**, 775 (1976).